J Mater Sci (2010) 45:811–817
DOI 10.1007/s10853-009-4004-8

Critical fluid shear stress analysis for cell–polymer adhesion

Aracely Rocha · Mariah Hahn · Hong Liang

Received: 29 July 2009 / Accepted: 29 October 2009 / Published online: 11 November 2009

Abstract A simple methodology to assess cell adhesion on materials was developed. We demonstrated that the cell adhesion strength could be quantified. Using this method, we were able to compare the NIH/3T3 Swiss mouse fibroblasts adhesion strength to poly(methyl methacrylate) and polycarbonate. A controlled fluid shear stress was applied to cells using a parallel plate rotational system. Cells detached from the surface in the radial direction. Results showed that there was a critical radius where the shear stress experienced by the cells equaled the cell adhesion strength. The cells outside this radius were removed while those inside maintained initial confluency. The quantitative evaluation of cell adhesion is beneficial for development of biomaterials.

Cell adhesion is considered one of the most important aspects of cytotoxicity [1] because it mediates cell–cell and cell–substrate interaction [2–8], cell shape, and cell function [1–4, 6, 7, 9]. Cytotoxicity tests have been conducted to understand how materials affect cell growth, shape, function, and adhesion. Such tests consist of exposing the biomaterial to live cells and biofluids that would surround the material when being used in the body. The live tissue or biofluids have been closely examined to evaluate damages caused by the material and/or its byproducts [1, 2, 10, 11]. Evaluation of the adhesion strength between cells and a biomaterial is a desirable method to assess cytotoxicity in vitro.

With the increase of applications and available materials, measuring cell adhesion has become critical for design and development of materials and devices for biological applications. The challenges are to develop a test procedure to quantify and compare cell adhesion over a wide spectrum of materials.

Several methods have been reported for measuring cell adhesion. They can be divided into the cell-to-cell and cell-to-substrate adhesion, or be separated into the single-cell and cell network adhesion. The most common method for analyzing average adhesion strength of a cell network to a substrate involves the application of defined levels of shear stress. The average cell adhesive force is the shear force at which cells are removed from the surface. Six different methods for shear stress testing have been reported: syringing [12, 13], centrifugation [14–16], channel flow [17–19], and rotational flow which includes rotational flow between a cone and a plate [18, 20–23], between parallel disks [24–26], or rotational flow over a plate [3, 27]. Among these, the rotational flow is considered to be the most reliable approach for studying the bulk cell adhesion [18]. Table 1 is a summary of shear flow techniques used in cell adhesion measurements. Although parallel plate systems have been reported [24, 25], the quantification of cell adhesion through shear stress has not been achieved.

In the present work, we focus on the cell-to-substrate adhesion. We propose a rheological approach in evaluating cell adhesion and in comparing various materials. During rotation, the shear stress varies with the radial position being the highest on the outside and zero at the center. The critical radius (R_C), shown in Fig. 1, is defined as the radius at which the cell adhesion force equals to the applied shear

A. Rocha · H. Liang (✉)
Department of Mechanical Engineering, Texas A&M University, 3123 TAMU, College Station, TX 77843-3123, USA
e-mail: hliang@tamu.edu

M. Hahn
Department of Bioengineering, Texas A&M University, 3120 TAMU, College Station, TX 77843-3123, USA

Table 1 Summary of cell adhesion studies performed from 1986 to 2004

Year (reference)	Test summary	Cell type	Substrate	Results
1986 [37]	Cells suspended in media	Human fibroblasts	Fibronectin coated glass	Maximum 80% cell adhesion
1989 [14]	Shear flow by centrifugal force	NIL cell fibroblasts	Fibronectin (F) and Tenascin (T) coated glass	$F_{max} = 40 \times 10^{-5}$ dynes/cell, $T_{max} = 2 \times 10^{-4}$ dynes/cell
1991 [25]	Rotating parallel disk shear flow	Endothelial cells	Tissue culture plate	Max 3×10^4 cells after 7 days
1993 [23]	Cone and plate rotational flow	Endothelial cells	Gelatin coated plate	Cell detachment begins at 40 s of applied stress
1994 [27]	Shear flow by rotating plate	Endothelial cells	Fibronectin coated plate	Visual observation of cells. No measurements
1997 [15]	Shear flow by centrifugal force	HT1080 human fibrosarcoma	HIV-1 coated glass	~10% cell attachment, independent of shear flow
1997 [24]	Impulse shear flow in rotating parallel disks	Neurons	Glass	0.53 cell strain at 800 dynes/cm^2 shear stress
1997 [3]	Shear flow by rotating plate	Rat osteosarcoma cells	Fibronectin coated glass	% remnant cells on surface
1998 [19]	Shear flow in channel	3T3 fibroblasts	Glass	0% attachment at 0.0068 dynes
2001 [13]	Jet impingement (impulse)	3T3 and L929 fibroblasts	Thermanox and stainless steel	Max 3T3 = 1060 dynes/cm^2 in thermanox. Max 929 = 1060 dynes/cm^2 on SS
2004 [17]	Shear flow in channel	WT NR6 fibroblasts	Fibronectin coated glass	Minimum 5% cell adhesion after 12 min at 4000 dynes/cm^2
2004 [6]	Shear flow in channel	Rat epitenon fibroblasts	PMMA	Flat surface ~190 cells. Rough surface ~100 cells attached

The reported results are generally qualitative and do not allow for comparison between materials or between cell types

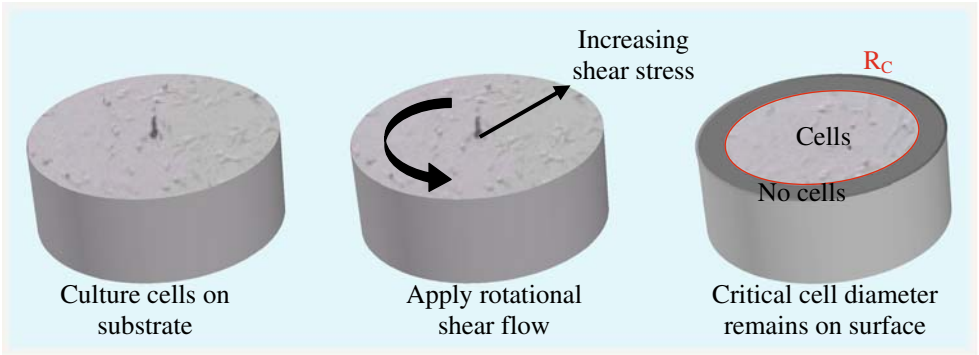

Fig. 1 Proposed approach. Critical shear stress is calculated with the critical radius. This is defined with the remaining surface cells after rotational shear stress testing

force. At this point, the cells are removed from the surface leaving a well-defined radius, which can be used to calculate the cell adhesion in terms of the shear stress to which the authors will refer as the critical shear stress (τ_C). Our proposed approach has the advantage of short test duration and low shear stress as compared to existing techniques.

In the present study, cell adhesion strength is investigated using a non-contacting parallel plate rheometer to apply a defined rotational shear to cell-seeded substrates. The parallel plates can be readily sterilized, and the rheometer can fit within standard laminar flow hoods. In addition, the maximum applied stress can be easily controlled with the rotational rheometer. The proposed methodology is validated by exploring the adhesion strength of NIH/3T3 fibroblasts, a commonly used cell type in adhesion studies [13, 21, 28, 29], on poly(methyl methacrylate) (PMMA) and polycarbonate (PC) substrates. These materials were selected because they had been used in biomedical applications [9, 29]. The success of this test relies on a laminar flow generated by the rotating plate. A laminar flow is one where the molecules in the flow move in smooth paths in well-defined concentric radii. A laminar

flow could be obtained by controlling the density of the testing liquid, the distance between plates, and the rotational velocity of the disk [24, 25, 30–32]. The goal of this research is to develop a methodology that quantitatively measures bulk cell adhesion such that it would allow for comparison between materials and between surface treatments. We ultimately intend to quantify the effects of surface roughness and surface treatments on the cell adhesion. The outcome of this research would enable us to adjust the surface properties of a material to potentially improve the tissue-implant adhesion.

A rotating rheometer (TA Instruments, AR-G2) was used to quantitatively evaluate cell adhesion to PC and PMMA surfaces by application of controlled maximum rotational shear. A Peltier plate was installed for temperature control. A parallel plate rheometer is mainly used to measure the viscoelastic properties of materials by shearing them between two circular parallel plates; one plate is fixed while the other rotates with a controlled shear stress, torque, or rotational speed. The AR-G2 rheometer used in this study was calibrated to compensate for rotational inertia and rotational bearing friction. It rotated with a magnetic (non-contact) motor on an air bearing decreasing friction and allowing higher system accuracy and more precise measurements. The rheometer was calibrated each time before testing and the error of the viscosity of water is less than 1%.

Twenty-four hours prior to material testing, mouse NIH/3T3 fibroblasts were seeded onto the material surface. The time duration was selected as a standard to ensure cell adhesion. Immediately prior to testing, the cell culture media was exchanged with physiological phosphate buffered saline. All tests were performed with a controlled maximum shear stress 37 °C. Two cell cultured samples of each material were tested and measurement was repeated for at least 6 times.

Substrate materials were cut into 3×3 cm^2. Their surface roughness was measured with a TR200 surface profilometer from Qualitest. The stylus scanned across the surface in a 5 mm single straight line in order to trace the surface profile and to measure the average surface roughness (R_a). As a standard procedure, five readings were taken at various locations and the average values of R_a were recorded. The samples were cleaned by rinsing in ethanol followed by air-drying in a laminar flow hood. They were then sterilized by shortwave UV irradiation for 24 h in a laminar flow hood and transferred to a sterile 6-well culture dish (Falcon). The surface roughness and contact angle of the PC and PMMA substrates were measured before and after sample preparation. A sterile Teflon ring with a 25 mm internal diameter was placed on top of each sample prior to cell seeding to avoid sample flotation.

Cell culture and cell seeding

NIH/3T3 fibroblasts (ATCC) were expanded in cell culture media (Dubelcco's Modified Eagles Medium supplemented with 10% bovine calf serum and penicillin/streptomycin) and maintained at 37 °C in 5% CO_2. All cell culture reagents were obtained from Cell Applications unless otherwise stated. Cells at passage 9–12 were harvested from T75 cell culture flasks and pelleted by centrifugation. The cells were resuspended in fresh cell culture media and counted using a hemacytometer. Cells were then seeded on each substrate at 5000 cells/cm^2. Cell density on sample was verified by cell count after 2 and 24 h of seeding.

The rheometer was fitted with a 25 mm diameter spindle. The PBS-immersed cell-seeded sample was placed on the lower, fixed plate, as shown in Fig. 2. The gap between the sample and the spindle was set to 480 μm, and the maximum shear stress was fixed for each sample (Table 2). Samples were exposed to shear for 10 min.

The samples were immersed in formalin for 24 h followed by dehydration in a series in graded ethanol baths to prepare for scanning electron microscopy (SEM). Formalin was used as a fixative to prevent the cells from moving. Although artifacts were introduced by the dehydration process, it was desirable to perform SEM imaging since many biomaterials were opaque and could not be readily observed by the standard transmission optical microscope.

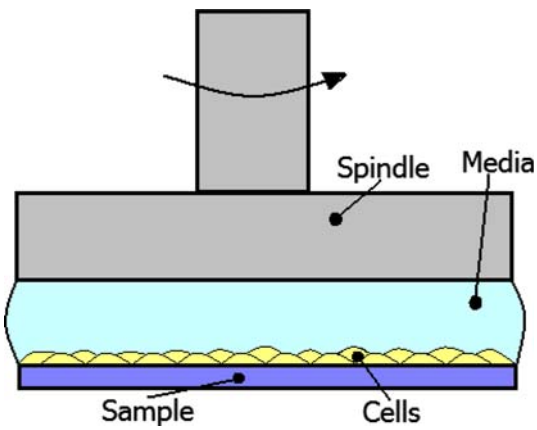

Fig. 2 Experimental setup. Sample with attached cells is placed on temperature control plate. The 25 mm diameter spindle is brought to a 480-μm gap from the sample. The liquid (media) used for testing is PBS

Table 2 Samples and controlled testing conditions

Sample	Maximum shear stress (Pa)	Gap (μm)	Testing time (min)	Temperature (°C)
PMMA	2.5	480	10	37
PC	1.0	480	10	37

Subsequently, samples were sputter-coated with gold and imaged with a JEOL JSM-6400 scanning electron microscope. The SEM images for PMMA were taken at 1000× magnification, with 15 kV accelerating voltage, and a working distance of 11 mm. The SEM images for PC were at 1000× magnification, 15 kV accelerating voltage, and 8 mm working distance. The pre-focus was done outside the test area to reduce the electron beam damage. Minor focus adjustments were done on the test area.

The surface roughness (R_a) and contact angle of the PC and PMMA samples before and after testing are summarized in Table 3. The R_a of PMMA had a 6.7% increase from 0.0672 to 0.0716 μm while PC had a 70% decrease from 0.0602 to 0.0182 μm. The surface of PC became smoother after testing. The contact angle increased by 1.1° for PC and decreased by 3.2° for PMMA.

Table 3 Surface roughness and contact angle before and after substrate exposure to ethanol and shortwave UV light

	R_a (μm)	Angle (°)
PC		
Before	0.067 ± 0.0254	71.3 ± 1.41
After	0.072 ± 0.0093	70.3 ± 3.21
PMMA		
Before	0.060 ± 0.0118	64.9 ± 2.51
After	0.018 ± 0.0075	68.1 ± 1.60

Figure 3 presents a representative set of images demonstrating the removal of cells beyond the radius of the critical shear stress for cells adhered to the PMMA exposed to a maximum rotational shear stress of 2.5 Pa. The circular region outlined in Fig. 3 corresponds to the critical radius, with associated optical micrographs positioned along its perimeter. Note that, beyond the critical radius, cells have been stripped from the surface while cells remain adherent within this radius. The PC was tested to a maximum of 1.0 Pa and it showed similar behavior, as evidenced by the SEM images in Fig. 4.

The measured R_C for PMMA and PC were 10.5 ± 0.15 mm and 6.36 ± 0.08 mm respectively. The observed R_C for each material was translated into critical shear stresses. Since the experiments were carried out at different maximum applied shear (τ_a) conditions, comparing the measured calculated values was necessary. The calculated R_C was 2.1 Pa for PMMA and 0.509 Pa for PC. The results are also summarized in Table 4.

Our results have shown that a critical shear radius (R_C) can be obtained with the experimental approach. The observed critical radius must be translated into a corresponding critical shear stress in order to make the experiments meaningful. To achieve this, it is necessary to examine the operation of the rheometer in more detail.

In the steady-shear operation, the spindle moves with a constant angular velocity, ω. The magnitude of ω is determined by the maximum shear stress. Assuming no slip

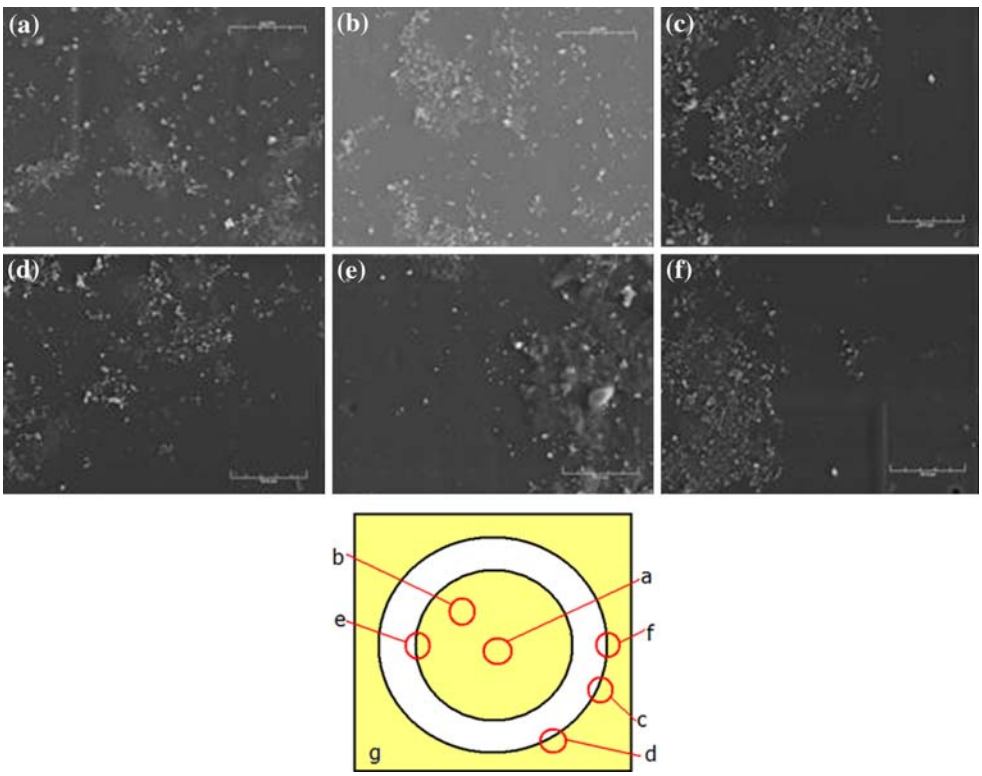

Fig. 3 *a–g* SEM images of PMMA after shear stress testing. The image locations are shown on the diagram above. The line scale on the SEM images is equivalent to 30 μm

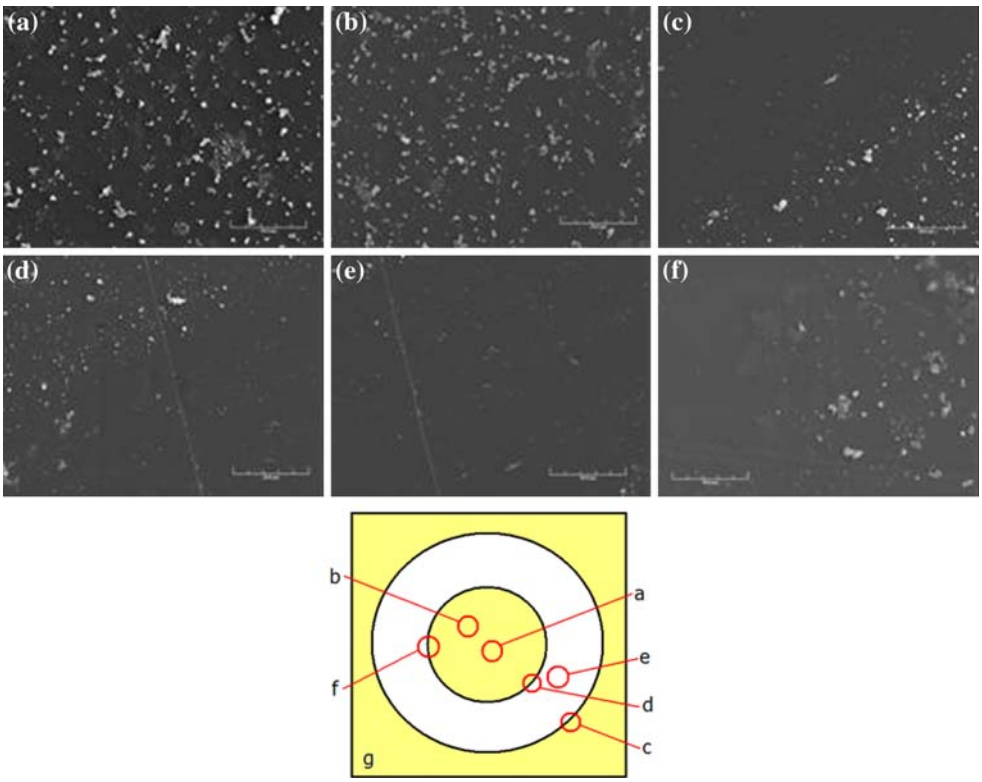

Fig. 4 *a–g* SEM images of PC after shear stress testing. The image locations are shown on the diagram above. The line scale on the SEM images is equivalent to 30 μm

Table 4 Results indicate that cells have a higher adhesion strength to PMMA than to PC

	Maximum shear stress (Pa)	Gap (μm)	Critical radius (mm)	τ_C (Pa)
PMMA	2.5	480	10.5 ± 0.15	2.10
PC	1.0	480	06.36 ± 0.08	0.509

at the interface, the relationship between the spindle azimuthal velocity (V_θ), the radial position (R), and the gap position (z) is linear, where r represents the spindle radius and Z the maximum gap as illustrated in Fig. 5:

$$V_\theta = \frac{\omega r z}{Z}, \quad 0 \le r \le R \quad 0 \le z \le Z \tag{1}$$

For a Newtonian fluid, the shear stress (τ) is

$$\tau = \eta \frac{dV_\theta}{dz}, \tag{2}$$

where η is the dynamic viscosity of the fluid and dV_θ/dz represents the change in azimuthal velocity with respect to the z-direction.

Combining Eqs. 1 and 2 yields,

$$\tau = \eta \frac{\omega R}{Z}, \quad 0 \le r \le R \tag{3}$$

Thus, for a Newtonian fluid undergoing non-slip rotational shear, τ is linearly related to radial position. Since ω is constant with radial position, ω at the critical radius, R_C must equal to ω at the spindle radius R ($\omega_{R_C} = \omega_R$):

$$\frac{Z}{\eta R_C}\tau_{R_C} = \frac{Z}{\eta R}\tau_{\max} \quad 0 \le r \le R \tag{4}$$

Thus,

$$\tau_{R_C} = \frac{\tau_{\max} R_C}{R} \tag{5}$$

Equation 5 was used to relate the observed critical radius to the critical shear stress. As shown in Figs. 3 and 4, the critical radius could be directly determined. Using Eq. 5, the critical shear stresses could be calculated. The results are summarized in Table 4. These results indicate that cell adhesion strength on PMMA is greater than on PC.

Our experiments have shown that the proposed approach was able to quantify the cell adhesion on different materials. The cells have a stronger adhesion to PMMA than to PC. There are potentially two reasons for this. One is the molecular interactions at the cell–substrate interface and the other is the surface roughness of the substrate. The molecular interactions are mainly due to the chemical composition of proteins and the substrate material. Cell attachment is mediated by the extracellular matrix (ECM), which is made of polysaccharides (sugars), and collagen (proteins) that provide structural support and protection to cells [33]. The proteins in the ECM are also responsible for carrying all necessary electrochemical

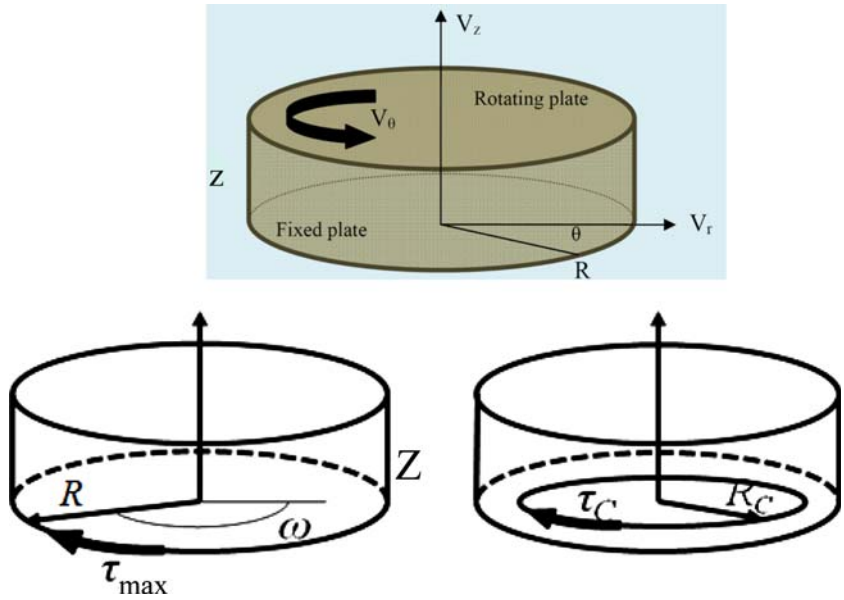

Fig. 5 Velocity (*V*) gradient in testing gap affects the shearing force experienced by the cells. (*Top*) Diagram of the media and the parameters affecting and controlling the laminar rotational flow. (*Bottom*) Visual interpretation of variables in Eqs. 4 and 5

processes and control tissue elasticity, humidity, and adhesion [34, 35]. Those are key elements in the cell/biomaterial interface [11]. The proteins that participate in cell–cell adhesion and cell–substrate adhesion vary by the cell type. In the case of fibroblasts, cytokines are the main proteins that mediate cell–cell adhesion while fibronectin is the main protein that controls cell–substrate adhesion in the ECM [9, 14, 33, 36]. The cell attaches to the fibronectin through the selectins. The end of the fibronectin that reacts with the selection on the fibroblast has a carboxylic end (–COOH). The other end has an amide group ($-NH_3^+$), which attaches to the substrate [37–41]. This amide group is electropositive, thus resulting in high adhesion strength if the surface is electronegative as in the case of PMMA. In terms of the surface roughness, our results showed that both samples had ultra smooth surface in comparison with the size of a cell ($\sim$30 μm). The PC became even smoother after the sample preparation. The wetting angle results showed that there was minimum change in the value ($\sim$3°) indicating the negligible effects of the surface roughness. The smooth surface enabled us to effectively evaluate the method to test cell/fluid shear. Further studies on roughness (at high value range) effects will be carried out in near future.

We developed a methodology, using a simple rheometry technique, to quantitatively measure the adhesive strength of cells attached to synthetic polymer surfaces. To demonstrate the technique, two polymer-based materials currently used in various biomedical applications were examined, namely PMMA and PC. The cell-seeded polymers were exposed to the rotational shear stress under a constant operating maximum shear stress constraint. Since a shear stress varies with its radial position, a threshold shear stress beyond which cells were detached from the material surface could be identified. Subsequent analysis of experimental results indicated that the cell adhesive strength on the tested materials varied based on material chemistry. One possibility for the PMMA to have a stronger adhesion than PC was due to its highly polarized C–H–O group.

The simple technique developed here will provide valuable information in estimation and understanding of cell–material adhesion. This method will allow us to quantify the cell adhesion strength to material surfaces with different properties. Using this approach it is possible to compare adhesion of cells to a wide spectrum of substrate materials.

Acknowledgements This research was in part sponsored by the NSF (0535578), the NSF–Louis Stokes Alliance for Minority Participation, Bridge-to-the-Doctorate Fellowship, the Texas A&M University, and the Texas Engineering Experiment Station (TEES). SEM analysis by Song Du, cell culture experiments assisted by Daniel Munoz Pinto, and support on TA Instruments by Sean Kohl are greatly appreciated.

References

1. Kirkpatrick CJ, Bittinger F, Wagner M, Kohler H, Van Kooten TG, Klein CL, Otto M (1998) Proc Inst Mech Eng 212:75
2. Piezzoferrato A, Ciapetti G, Stea S, Cenni E, Arciola CR, Granchi D, Savarino L (1994) Clin Mater 15:173
3. Garcia AJ, Ducheyne P, Boettiger D (1997) Biomaterials 18:1091
4. Hu L, Zhang X, Miller P (2006) J Appl Phys 100:84701
5. Puecha PH, Poole K, Knebelc D, Muller DJ (2006) Ultramicroscopy 106:637
6. Martines E, McGhee K, Wilkinson C, Curtis A (2004) IEEE Trans Nanobiosci 3:90
7. Curtis ASG, Lackie JM (1991) Measuring cell adhesion. Wiley, New York
8. Anderson AA (2005) Math Med Biol 22:163

9. Yamamoto A, Mishima S, Maruyama N, Sumita M (2000) J Biomed Mater Res 50:114
10. Sivakumar R (1999) Bull Mater Sci 22:647
11. Dee KC, Puleo DA, Bizios R (2002) An introduction to tissue-biomaterial interactions. Wiley, Hoboken, NJ
12. Bongrand P, Claesson PM, Curtis ASG (1994) Studying cell adhesion. Springer-Verlag, Heidelberg
13. Bundy KJ, Harris LG, Rahn BA, Richards RG (2001) Cell Biol Int 25:289
14. Lotz MM, Burdsal CA, Erickson HP, McClay DR (1989) J Cell Biol 109:1795
15. Channavajjala LS, Eidsath A, Saxinger WC (1997) J Cell Sci 110:249
16. Tateishi T, Ushida T (1995) Cell adhesion strength to bioceramics and morphology, Southern biomedical engineering conference, Proceedings, 14th Southern biomedical engineering conference, April 7–9, 1995. Louisiana State University Medical School, IEEE, Biomedical Research Foundation of Northwest Louisiana, pp 278–281
17. Lu H, Koo LY, Wang WM, Lauffenburger DA, Griffith LG, Jensen KF (2004) Analyt Chem 75:5257
18. Brown TD (2000) J Biomech 33:3
19. Ming F, Whish WJD, Hubble J, Eisenthal R (1998) Enzyme Microb Technol 22:94
20. Buschmann MH, Dieterich P, Adams NA, Schnittler HJ (2005) Biotechnol Bioeng 89:493
21. Blackman BR, Barbee KA, Thibault LE (2000) Ann Biomed Eng 28:363
22. Malek AM, Ahlquist R, Gibbons GH, Dzau VJ, Izumo S (1995) Meth Cell Sci 17:165
23. Raposo S, Lima-Costa ME (2006) Biotechnol Lett 28(6):431
24. LaPlaca MC, Thibault LE (1997) Ann Biomed Eng 25:665
25. Ono O, Ando J, Kamiya A, Kuboki Y, Yasuda H (1991) Cell Struct Funct 16:365
26. Horbett TA, Waldburger JJ, Ratner BD, Hoffman AS (1998) J Biomed Mater Res 22:383
27. Reutelingsperger CPM, Van Gool RGJ, Heijnen V, Frederik P, Lindhout T (1994) J Mater Sci Mater Med 5:361
28. Hallab NJ, Bundy KJ, O'Connor K, Moses RL, Jacobs JJ (2001) Tissue Eng 7:55
29. Alonso S, Lau J, Jaber BL (2008) Biocompatible hemodialysis membranes for acute renal failure (review). In: Cochrane database of systematic reviews. Wiley, New York, pp 1–38
30. Ando J, Nomura H, Kamiya A (1987) Microvasc Res 33:62
31. Oliveira LA, Pecheux J, Restivo AO (1991) Theor Comput Fluid Dyn 2:211
32. Papadaki M, McIntire LV (1999) Tiss Eng Methods Protocols 18:577
33. Hahn LHE, Yamada KM (1979) Cell 18:1043
34. Pollard TD, Earnshaw WC (2002) Cell biology. Sounders, Philadelphia, PA
35. Alberts B, Bray D, Lewis J, Raff M, Roberts K, Watson JD (1994) Molecular biology of the cell. Garland Publishing, New York
36. Woods A, Couchman JR, Johansson S, Hook M (1986) EMBO J 5:665
37. Biren CA, Barr RJ, McCullough JL, Black KS, Hewitt CW (1986) J Invest Dermatol 86:611
38. Horbett TA, Schway MB (1988) J Biomed Mater Res 22:763
39. Gumbiner BM (1996) Cell 84:345
40. Keselowsky BG, Collard DM, Garcia AJ (2003) J Biomed Mater Res 66:247
41. Underwood PA, Steele JG, Dalton BA (1993) J Cell Sci 104:793